Swansea University
Prifysgol Abertawe

Cronfa
Setting Research Free

Cronfa - Swansea University Open Access Repository

_____

This is an author produced version of a paper published in :
Metallurgical and Materials Transactions A

_____

Cronfa URL for this paper:

http://cronfa.swan.ac.uk/Record/cronfa29679

_____

_____

A Statistical Test for Identifying the Number of Creep Regimes when using the Wilshire Equations for Creep Property Predictions

MARK EVANS

College of Engineering, Swansea University, Bay Campus, Engineering East, Fabian Way, Crymlyn Burrows, Swansea, SA1 8EN, Wales UK.

Tel: +44(0)1792 295748; Fax: +44(0)1792 295676; Email: m.evans@swansea.ac.uk

ABSTRACT

A new parametric approach, termed the Wilshire equations, offer the realistic potential of being able to accurately life materials operating at in service conditions from accelerated test results lasting no more than 5,000h. The success of this approach can be attributable to a well-defined linear relationship that appears to exist between various creep properties and a log transformation of the normalised stress. However, these linear trends are subject to discontinuities, the number of which appears to differ from material to material. These discontinuities have until now been i. treated as abrupt in nature and ii. been identified by eye from an inspection of simple graphical plots of the data. This paper puts forward a statistical test for determining the correct number of discontinuities present within a creep data set and a method for allowing these discontinuities to occur more gradually - so that the methodology is more in line with the accepted view as to how creep mechanism evolve with changing test conditions. These two developments are fully illustrated using creep data sets on two steel alloys. When these new procedures are applied to these steel alloys, not only do they produce more accurate and realistic looking long-term predictions of the minimum creep rate but they also lead to very different conclusions about the mechanisms determining the rates of creep from those originally put forward by Wilshire.

Keywords:

Minimum creep rate, Wilshire methodology, Statistical testing, Threshold models

I. INTRODUCTION

To reduce fuel consumption and CO2 emissions from power plants, new high-temperature alloys are required to resist the increase in temperature and pressure needed to raise plant efficiencies. However, at the design stage, information must be available on the stresses to which multiple batches of these new alloys can sustain without creep fracture occurring within 100,000h at the service temperatures [1]. Unfortunately, with the traditional parametric, numerical and computational methods, long term strengths cannot be predicted by extrapolation of short-term property sets. Consequently, at present, protracted and expensive long-duration test programmes are necessary to determine the 100,000h creep rupture

39 strengths, with a reduction in this 12 to 15 year "materials development cycle" being defined
40 as the No.1 priority in the 2007 UK Energy Materials-Strategic Research [2].

41   In response to this problem, over recent years, a new approach - termed the Wilshire
42 equations - has been devised which appears to allow accurate long-term strength values to be
43 obtained by extrapolation from accelerated short-term measurements. The last 5 to 6 years has
44 seen the appearance in the literature of this methodology applied to a wide range of materials
45 used for high temperature application in the power generation and aerospace industries in an
46 attempt to verify the validity and accuracy of this approach [3-8]. Specifically, 100,000h strength
47 estimates have been produced by analysis of multi-batch data lasting up to only 5,000h for a
48 series of ferritic bainitic and martensitic steels for power and petrochemical plant and titanium
49 alloys used in aero engine blades and disc.

50   The Wilshire equation takes the form,

51
$$(\sigma/\sigma_{TS}) = \exp\left\{-k_2\left[\dot{\varepsilon}_m.\exp(Q_c^*/RT)\right]^v\right\}$$
[1a]

52 where $\dot{\varepsilon}_m$ is the minimum creep rate, T is the absolute temperature, σ the stress, σ_{TS} the tensile
53 strength, R the universal gas constant, Q_c^* the activation energy for self-diffusion and where
54 k_2 and v are further model parameters. This equation provides a sigmoidal data presentation
55 such that $\dot{\varepsilon}_m \to \infty$ as $(\sigma/\sigma_{TS}) \to 1$ (provided $v < 0$), whereas $\dot{\varepsilon}_m \to 0$ as $(\sigma/\sigma_{TS}) \to 0$. Wilshire
56 and Battenbough [3] proposed a very similar expression to Eq. [1] for the stress and temperature
57 dependencies of the time to failure, t_f, and time to various different strains. The parameters k_2
58 and v appear to be dependent upon stress (and possibly temperature) for many steel alloys.

59   This approach can be contrasted to the traditional power law expression for modelling
60 creep properties as a function of stress and temperature

61
$$\dot{\varepsilon}_m = A\sigma^n\exp(Q_c^*/RT)$$
[1b]

62 but once again the unknown parameter (Q_c^* and n) change with test conditions. In this approach
63 the variation in n and Q_c^* with test conditions is traditionally explained in terms of differing
64 creep mechanisms being dominant at different stresses and temperatures. For example, a
65 transition from $n \approx 4$ to $n \approx 1$ is traditionally taken as evidence of a change from dislocation to
66 diffusional creep processes as stress diminishes. Likewise, when creep occurs by diffusion
67 controlled generation and movement of dislocations a fall in the activation energy below that
68 associated with lattice self-diffusion is interpreted either as i. deformation behaviour being
69 increasingly controlled by preferential diffusion along dislocation cores at low temperatures
70 within a high stress regime, or by ii. deformation behaviour being increasingly controlled by
71 stress directed vacancy flow along grain boundaries at low temperatures and stresses.

72   However, the results obtained from using Eq. [1a] have lead authors like Wilshire and
73 Scharning [4] and Wilshire and Whittaker [5] to suggest that the parameter instability observed
74 in k_2 and v is not the result of a change from dislocation to diffusional creep processes. Instead,
75 and depending on the material under investigation, they choose to interpret the observed
76 changes in k_2 and v as either being:

77
78   i.   the result of particle coarsening associated with long test durations at lower stresses.
79   ii.   or as a result of a change from creep occurring from the generation of new dislocations
80   within the lattice structure itself to creep occurring from the movement of dislocations pre-
81   existing only in the grain boundary zones as a result of a low stress level.
82

83   The fact that Eq. [1a] has been remarkably successful in being able to predict creep
84   lives at operating conditions from highly accelerated tests of very short duration and over a
85   wide range of materials is taken by these authors to be strong evidence to support this view.

86   As an illustration of this point of view consider two steel alloys. Fig.1a summarises the
87   results obtained by Wilshire and Scharning[4] in their 2007 study of 1Cr - 1Mo - 0.25V steel
88   using the NIMS[9] data base on this material. As can be seen from this figure, there appears to
89   be one break point (and therefore two creep regimes) where the values for k_2 and v change, but
90   according to the authors, the activation energy remains unchanged. By studying the
91   metallographic evidence obtained by NIMS [10], the authors found that little or no change was
92   observed in the as received bainitic microstructures when hardness reductions were small,
93   whereas distinguishable increases in carbide size was apparent when the hardness values fell
94   of rapidly. Furthermore, only very modest falls in hardness were observed in the high
95   normalised stress range, with rapid harness reductions occurring the low normalised stress
96   ranges. Thus, the unchanging activation energy quoted by the authors is taken to mean that
97   creep is determined by behaviour within the crystal lattice. Then the changes in k_2 and v reflect
98   differences in the rates of creep strength reduction caused by the evolution of the tempered
99   bianitic microstructure in the low normalised stress range. This causes creep rates to be much
100   higher in the low stress regime than would be predicted by relations prevalent at higher stresses.

101   Thus in Fig.1a the larger carbide particle sizes present at very low stresses (where the
102   test duration is long), means that at a given stress, creep rates will be greater than that predicted
103   from relations that hold at higher stresses. Hence the steeper slope of the best fit line shown in
104   Fig.1a below a normalised stress of around 0.4. Despite this, and as clearly seen in Fig. 1a, the
105   presence of these distinctly different stress regimes does not prevent the accurate prediction of
106   creep lives out to over 100,000 hours using only data up to 5,000h for the purpose of parameter
107   estimation.

108   In their study of 2.25Cr-1Mo steel, Wilshire and Whittaker [5] identified three different
109   values for v and k_2 that corresponded to high, medium and low stress regimes – as seen in Fig.
110   1b for the MAF batch of materials within the NIMS[11] data base on this steel alloy. For this
111   material, these authors again suggest that no transition takes place from dislocation to
112   diffusional creep with decreasing applied stress. Instead, dislocation creep processes are rate
113   controlling at all stress levels, even though the detailed dislocation processes vary in different
114   stress regimes. Thus, with 2.25Cr-1Mo steels, the creep and creep fracture properties differ
115   above and below $\sigma \approx \sigma_Y$ (where σ_Y is the yield stress). According to Wilshire and Whittaker
116   [5], when $\sigma > \sigma_Y$, so that the initial strain on loading has both elastic and plastic components,
117   creep is controlled by the generation and movement of dislocations within the grains where the
118   activation energy is highest.

In contrast, when $\sigma < \sigma_Y$, so that the strain on loading has essentially only an elastic component, new dislocations are not generated within the grains. Instead, creep occurs within the grain boundary zones, i.e. by grain boundary sliding or diffusion along existing dislocations and grain boundaries with associated deformation in the grain regions adjacent to the boundaries (where the activation energy is lower). Hence, the creep rates when $\sigma < \sigma_Y$ are slower and the creep lives are longer than expected by direct extrapolation of $\dot{\varepsilon}_m$ data obtained when $\sigma < \sigma_Y$. Another change in creep and creep rupture behaviour occurs when σ approximately equals $0.2\sigma_{TS}$. With this material, the original ferrite/bainite microstructure degrades to ferrite and molybdenum carbide particles in long term tests at the highest creep temperatures, with very coarse carbide particles forming along the grain boundaries. This carbide coarsening reduces creep strength in the matrix allowing diffusion to occur within the grains once again where the activation energy is higher. In these cases, because of the loss of creep resistance caused by this transformation, the $\dot{\varepsilon}_m$ values are larger when $\sigma < 0.2\sigma_{TS}$ than would be predicted by extrapolation of data collected at intermediate σ levels. These authors have provided similar explanations for the observed breaks in other power generating materials as well.

Yet despite the simplicity of these types of explanation, and the accuracy of predictions of creep life made using this approach, the methodology has always been presented (with Figs .1a,b being a typical visualisation of the approach in the literature) showing an abrupt change in parameter values at precise values for the normalised stress. This suggests that at this normalised stress the cause of creep deformation suddenly changes from being 100% controlled by dislocations within the bulk to 100% determined by dislocations within the boundaries. Yet, such changes are known to occur gradually, with a gradual transition say from deformation being controlled by the bulk to being controlled within the grains as stress falls below a critical value.

This paper therefore has two main aims designed to enhance and further formulise the Wilshire methodology. The first is to modify the Wilshire methodology to allow for a gradual rather than abrupt change by using the approach first put forward by Evans[12] - but to generalise this approach to allow for more than one "regime" change. Secondly, a statistical test is presented that enables the number of regime changes or breaks present in the creep data to be determined. Such a statistical test is not as straight forward as it first sounds because under the null hypothesis of no regime change some of the parameters in the Wilshire equations are not actually defined. As a consequence of this, the distribution of any test statistic for this null hypothesis is non-standard - as maximum likelihood (or least squares) theory is no longer directly applicable. Interestingly, the modified Wilshire methodology proposed here provides a neat solution to this problem of testing for regime change.

II. THE MODIFIED WILSHIRE EQUATIONS

A.   Two Competing Creep Deformation Mechanisms

157   To develop the proposed modification of the Wilshire equations, it is first helpful to
158   rewrite Eq. [1a] in the following way

159    $$y = a + bx_1 + dx_2 + u_1 \qquad [2]$$

160   with y being the natural log of the minimum creep rate, $x_1 = \ln[-\ln(\sigma/\sigma_{TS})]$ and $x_2 = 1/RT$, $b =$
161    $1/v$, $a = \ln[k_2/v]$ and $d = Q^*_c$. u_1 are the residuals included in the specification to make clear the
162   fact that the experimental data on creep properties are stochastic in nature. Estimation
163   procedures for determining values for a, b and d typical take the form of minimising the sum
164   of these squared residuals. Consider next the simplest scenario where the data has at most just
165   a single break or two distinct creep mechanisms or regimes. In such a situation Eq. [2] can be
166   written as

167    $$y = \begin{array}{ll} a_1 + b_1 x_1 + d_1 x_2 + u_2 & \text{with proportion } 1 - w \\ a_2 + b_2 x_1 + d_2 x_2 + u_2 & \text{with proportion } w \end{array} \qquad [3a]$$

168   where, for example, b_1 is the value for b under one creep mechanism and b_2 the value for b
169   under the other creep mechanism. u_2 are the residuals associated with the Wilshire model that
170   has two creep regimes. The value for w determines how much of the overall minimum creep
171   rate is determined by a particular mechanism. So when $w = 0.5$ two different creep processes
172   (for example dislocation movements within grain boundaries versus dislocation movements
173   within the bulk) contribute equally towards the overall minimum creep rate. Then as w tends
174   to unity (and so $1 - w_1$ tends to zero) the creep rate is increasingly determined by just one of
175   these creep mechanisms. When $w = 1$, the creep rate is determined 100% by a single
176   mechanism. In effect w measures the dominance of a particular deformation mechanism. Then
177   d_1 can be interpreted as the activation energy associated with the first mechanism, and d_2 is the
178   activation energy associated with the other mechanism (for example the activation energies
179   associated with dislocation movements within boundaries and within the bulk). In comparison
180   to Eq. [1], $b_1 = 1/v_1$ and $b_2 = 1/v_2$ where v_1 and v_2 are the values for v in Eq. [1] associated with
181   the two different regimes. Likewise, $a_1 = \ln[k_{21}/v_1]$ and $a_2 = \ln[k_{22}/v_2]$ where k_{21} and k_{22} are
182   the values for k_2 in Eq [1] associated with the two different regimes.

183   Whilst it is unclear exactly how w varies with the normalised stress, it must be the case
184   that w tends 1 as σ/σ_{TS} increases. Whilst this could happen in a linear fashion, a more general
185   representation would allow for a non-linear transition between the regimes

186    $$w = \frac{1}{1 + \exp[-\beta_1(x_1 - x_1^*)]} \qquad [3b]$$

187   where x_1^* is some critical value for the normalised stress, namely that normalised stress where
188   creep rates are equally governed by the two competing mechanisms (i.e. where $w = 0.5$). The
189   specification given by Eq. [3a,b] is very similar to threshold models used quite commonly for
190   modelling time series data and the reader is referred to Tong [12] and Martin et. al. [13] for a good
191   review on how to identify and estimate the parameters of such models. Writing the
192   determination of w in this way has the clear advantage that the traditional Wilshire equation

193 can be recovered from this re-specification. That is, if β_1 is large (typically larger than 500),
194 the S shaped sigmoidal curve given by Eq. [3b] becomes extremely steep around x^*_1 and
195 essentially appears as a step like function at this point leading to a very abrupt regime change
196 – which is how the Wilshire equations has been applied up until now. That is, as β_1 increase,
197 Eq. [3b] approximates to the step function

198
$$w = \begin{cases} 1 & \text{if } x_1 \geq x^*_1 \\ 0 & \text{if } x_1 < x^*_1 \end{cases} \qquad [3c]$$

199 However, the main advantage if Eq. [3b] is that unlike a step function implied by the
200 traditional Wilshire model, w is differentiable and this provides a means for statistically testing
201 whether such a regime change exists in the first place.

202 Eqs. [3a,b] or Eq. [3a,c] can be combined into a single equation of the form

203
$$y = (a_1 + b_1 x_1 + d_1 x_2 + u_2)(1 - w) + (a_2 + b_2 x_1 + d_2 x_2 + u_2)w$$

204 or

205
$$y = a_1 + b_1 x_1 + d_1 x_2 + (a_2 - a_1)w + (b_2 - b_1)wx_1 + (d_2 - d_1)wx_2 + u_2 \qquad [3d]$$

206

207 When the model is expressed as in Eq. [3d], a simple estimation procedure for the
208 unknown parameters can be used. First, arbitrarily choose a value for β_1 and x^*_1 in Eq. [3b].
209 This makes w an observable variable in Eq. [3d] so that the parameters of this equation can be
210 obtained by regressing y on a constant, x_1, x_2, w and the cross products wx_1 and wx_2 (this is
211 just multiple linear least squares the value for u^2_2 summed over all data points is minimised).
212 Then a grid search can be carried out to find the values for β_1 and x^*_1 that further minimise the
213 residual sum of squares (x^*_1 will typically be varied in small increments over the range 0.2 to
214 0.8, whilst β_1 will typically be varied in less small increments over the range 0 to 1000). This
215 will produce estimates for a_1, b_1 and d_1 together with a_2-a_1, b_2-b_1 and d_2-d_1. From all these
216 estimates, it is then possible to recover the values for a_2, b_2 and d_2.

217 *B.   Three or More Competing Creep Deformation Mechanisms*

218 There are a number of ways to generalise Eq. [3d]. One is to allow for mechanism
219 changes at more than one normalised stress level - as suggested by Wilshire and Whittaker
220 when studying data on 2.25Cr-1Mo steel. The second is to allow the mechanism to change at
221 various stress and temperature levels as is typically portrayed in traditional creep deformation
222 maps. Such an approach was considered by Evans[14] and will not be discussed further in this
223 paper. In the former approach, Eq. [3a] would generalise to

224
$$y = \begin{matrix} a_1 + b_1 x_1 + d_1 x_2 + u_3 \\ a_2 + b_2 x_1 + d_2 x_2 + u_3 \\ a_3 + b_3 x_1 + d_3 x_2 + u_3 \\ \vdots \\ a_p + b_p x_1 + d_p x_2 + u_3 \end{matrix} \quad \begin{matrix} \text{with proportion } w_1 \\ \text{with proportion } w_2 \\ \text{with proportion } w_3 \\ \vdots \\ \text{with proportion } w_p = 1 - w_1 - w_2 - .. - w_{p-1} \end{matrix}$$

225
$$[4a]$$

226 where u_3 are the residuals when there are p different creep mechanisms that predominantly
227 come into operation at p - 1 different normalised stresses. For example, consider three possible
228 creep regimes that occur within different normalised stress ranges. The Eq. [4a] simplifies to

229 $y = (a_1 + b_1 x_1 + d_1 x_2 + u_3)(w_1) + (a_2 + b_2 x_1 + d_2 x_2 + u_3)(1 - w_1 - w_3) + (a_3 + b_3 x_1 + d_3 x_2 + u_3)w_3$

230 or

231
$$y = a_2 + b_2 x_1 + d_2 x_2 + (a_1 - a_2)w_1 + (a_3 - a_2)w_3 + (b_1 - b_2)w_1 x_1 + (b_3 - b_2)w_3 x_1$$
$$+ (d_1 - d_2)w_1 x_2 + (d_3 - d_2)w_3 x_2 + u_3 \qquad [4b]$$

232 with

233
$$w_1 = 1 - \frac{1}{1 + \exp[-\beta_1(x_1 - x_1^*)]}; \quad w_3 = \frac{1}{1 + \exp[-\beta_3(x_1 - x_1^{**})]}; \quad w_2 = 1 - w_1 - w_3 \qquad [4c]$$

234 and with x_1^{**} being the normalised stress associated with another creep mechanism starting to
235 dominated the process of deformation. Eq. [4c] allows the intermediate regime to phase in as
236 the regimes either side start to take on a less dominant role.

III. A STATISTICAL TEST FOR REGIME CHANGE

238 *A. Two Competing Creep Deformation Mechanisms*

239 By testing jointly that the parameters $(a_2 - a_1)$, $(b_2 - b_1)$ and $(d_2 - d_1)$ are all equal to zero
240 in Eq. [3d] it becomes possible to determine statistically how many regime changes are present
241 within the experimental data. A natural test statistic to determine whether or not these are zero
242 (which is the null hypothesis) is to jointly test whether the parameters in front of w, wx_1 and
243 wx_2 in Eq. [3d] are significantly different from zero. (Readers are referred to Vining and
244 Kowalski [15] for a description on this joint test of significance). However, the Standard F test
245 normally constructed to carry out such a test, no longer has an F distribution because the
246 parameters β_1 and x_1^* in Eq. [3b] are not defined under this null hypothesis and so conventional
247 maximum likelihood theory is no longer directly applicable. An alternative approach is to test
248 $\beta_1 = 0$ as w is Eq. [3b] then becomes a constant resulting in Eq. [3a] collapsing to Eq. [1].
249 However, in this case it is the parameters x_1^*, a_1, b_1, d_1, a_2, b_2 and d_2 that are not identified under
250 the null hypothesis. In the Econometrics literature, three possible ways to address this problem
251 have been identified. Luukkonen, Saikkonen and Terasvirta [16] suggest focusing on the local
252 asymptotics at $\beta_1 = 0$. This approach has the advantage of yielding a test statistic with a standard
253 distribution under the null hypothesis. Alternatively, Hansen [17] proposes a solution based on

254 local asymptotics at $a_1 = b_1 = d_1 = a_2 = b_2 = d_2 = 0$, which yields a test statistic whose distribution
255 must be approximated by bootstrapping. Lee, Granger and White [18] proposes a test similar to
256 Hansen's in that it tests $a_1 = b_1 = d_1 = a_2 = b_2 = d_2 = 0$. However, it draws simulated values for
257 x^*_1 and β_1 to generate values for w in Eq. [3b]. The authors suggest using a rectangular
258 distribution to do this simulation.

259 This paper makes use of the first of these approaches. Let $z = \beta_1(x_1 - x^*_1)$ so that under
260 the null hypothesis of no regime change $\beta_1 = 0$, and so $z = 0$. The first three derivatives of Eq.
261 [3b] with respect to z, evaluated at $z = 0$ are as follows:

262
$$w_0^{(1)} = \left.\frac{\partial w}{\partial z}\right|_{z=0} = \left.\frac{\exp(-z)}{(1+\exp(-z))^2}\right|_{z=0} = \frac{1}{4}$$

263
$$w_0^{(2)} = \left.\frac{\partial^2 w}{\partial z^2}\right|_{z=0} = \left.\frac{\exp(-z) - \exp(-2z)}{(1+\exp(-z))^3}\right|_{z=0} = 0$$

264
$$w_0^{(3)} = \left.\frac{\partial^3 w}{\partial z^3}\right|_{z=0} = \left.\frac{\exp(3z) - 4\exp(2z) + \exp(z)}{6\exp(2z) + 4\exp(3z) + \exp(4z) + 4\exp(z) + 1}\right|_{z=0} = -\frac{1}{8}$$

265 Using these derivatives in a third order Taylor series expansion of w around $z = 0$ gives

266
$$w \approx w_{(0)} + w_0^{(1)}(z-0) + \frac{1}{2}w_0^{(2)}(z-0)^2 + \frac{1}{6}w_0^{(3)}(z-0)^3 = \frac{1}{2} + \frac{1}{4}z + 0 - \frac{1}{48}z^3 \quad [5a]$$

267 Now the expansion of z^3 in Eq. [5a] has terms x_1, x^2_1 and z^3_1 so that this function can
268 be approximated by the cubic

269
$$w \approx \delta_0 + \delta_1 x_1 + \delta_2 x_1^2 + \delta_3 x_1^3 \qquad [5b]$$

270 This Taylor series approximation represents the local behaviour of the function in the
271 vicinity of $\beta_1 = 0$ and therefore provides a basis for a test of regime change. Substituting Eq.
272 [5b] into Eq. [3d], (and ignoring the residual term for the moment), gives a regression equation
273 of the form

274
$$\begin{aligned} y = &\{a_1 + (a_2 - a_1)\delta_0\} + \{b_1 + (a_2 - a_1)\delta_1 + (b_2 - b_1)\delta_0\}x_1 + \{d_1 + (d_2 - d_1)\delta_0\}x_2 \\ &+ \{(a_2 - a_1)\delta_2 + (b_2 - b_1)\delta_1\}x_1^2 + \{(a_2 - a_1)\delta_3 + (b_2 - b_1)\delta_2\}x_1^3 + (b_2 - b_1)\delta_3 x_1^4 \quad [5c] \\ &+ (d_2 - d_1)\delta_1 x_1 x_2 + (d_2 - d_1)\delta_2 x_1^2 x_2 + (d_2 - d_1)\delta_3 x_1^3 x_2 \end{aligned}$$

275 Under the null hypothesis of no regime change, there are no interaction terms and no
276 quadratic, cubic or fourth order terms (as the values in round brackets are then zero) present in
277 Eq. [5c]. Therefore, the steps required to perform a test of the null hypothesis that there is just
278 one creep mechanism (i.e. no creep regime change) are as follows:

279 Step 1: Regress y on $\{1, x_1, x_2\}$ (i.e. assuming no regime change as in Eq. [2]) to get estimates
280 of the residuals u_1 shown in Eq.[2].

281   Step 2: Regress u_1 on $\{1, x_1, x_2, x^2_1, x^3_1, x^4_1, x_1x_2, x^2_1x_2, x^3_1x_2\}$.

282   Step 3: Compute the Lagrange multiplier statistic $LM = NR^2$ where N is the sample size and
283   R^2 is the coefficient of determination from the regression carried out in step 2. Under the null
284   hypothesis that $\beta_1 = 0$ (i.e. no regime change), LM is asymptotically distributed as a chi square
285   variable with 6 degrees of freedom.

286   The intuition behind this test is that any important regime change excluded from the
287   regression in step 1 will show up in the regression carried out in step 2 in the form of a high
288   value for the coefficient of determination R^2 (and so lead to a large chi square variable and the
289   subsequent rejection of the null hypothesis).

290   *B.   Three or More Competing Creep Deformation Mechanisms*

291   This test is easily generalised to three or more competing mechanism by adopting a
292   sequential estimation and testing procedure. Thus, the initial null hypothesis is for a linear
293   model with a single creep mechanism and this is tested against the alternative of a model with
294   a single regime change (or two mechanisms) using exactly the same procedure as that outlined
295   in sub section IIIA above. If the null hypothesis is accepted that is the end of this sequential
296   procedure and there is just a single creep mechanism present within the data. If the null
297   hypothesis is rejected at significance level α (where typically α is taken to be 5%), the new
298   null hypothesis becomes a model with two creep regimes present and this is tested against the
299   alternative of a model with three regime changes, using once again a three step procedure. That
300   is:

301   Step 1: Regress y on $\{1, x_1, x_2, w_1, wx_1, w_1x_2\}$ (i.e. assuming one regime change as in Eq, [3d])
302   to get estimates of the residuals u_2 shown in Eq. [3d].

303   Step 2: Regress u_2 on $\{1, x_1, x_2, w_1, wx_1, w_1x_2, x^2_1, x^3_1, x_1x_2, x_1x^2_1, x_1x^3_1, x^3_1x_2\}$.

304   Step 3: Compute the Lagrange multiplier statistic $LM = NR^2$ where N is the sample size and
305   R^2 is the coefficient of determination from the regression carried out in step 2. Under the null
306   hypothesis of one regime change, LM is asymptotically distributed as a chi square variable
307   with 6 degrees of freedom. Accept the model with three different creep regimes if the null
308   hypothesis is rejected at significance level $\tau\alpha$, $0 < \tau < 1$. Reducing the significance level
309   compared to the preceding test favours parsimonious models. Choosing τ is left to the modeller,
310   but $\tau = .5$ is a common choice.
311

312   This sequential estimation and testing is continued until the first acceptance of the null
313   hypothesis. This yields the specification for the final model and determines the number of creep
314   mechanisms generating the experimental creep data.
315

316   # IV. APPLICATIONS

317   *A.   1Cr - 1Mo - 0.25V Steel*

318   In order to apply the sequential testing procedure described in section III above to the
319   1Cr - 1Mo - 0.25V data shown in Fig. 1a, it is necessary to first construct the residuals u_1 in
320   Eq. [2]. Columns 2 and 3 of Table I show the estimates made for the parameters in Eq. [2]. The
321   t values show that all the parameters are statistically significant at the 1% significance level
322   with the value for d implying an activation energy of just over 300kJmol^{-1}. These estimates
323   imply that the residuals u_1 are given by

324        $u_1 = y - (23.2390 - 6.9101x_1 - 304.4505x_2)$ [6a]

325   The second and third columns of Table II show the results obtained when u_1 is regressed
326   on $\{1, x_1, x_2, x^2{}_1, x^3{}_1, x^4{}_1, x_1x_2, x^2{}_1x_2, x^3{}_1x_2\}$ for the second step of the three step test procedure.
327   It reveals that the parameter in front of x_1x_2 in Eq. [5c] is statistically different from zero at the
328   5% significance level. Eq. [5c] also suggests that this can only be so if there is a statistically
329   significant change in the activation energy (as then $d_2 - d_1 \neq 0$). This part of Table II also reveals
330   that the parameter in front of x_1 in Eq. [5c] is statistically different from zero at the 5%
331   significance level. Again, Eq. [5c] also suggests that this can only be so if there is a statistically
332   significant change in either b_1 or a_1 or both, as then $b_2 - b_1 \neq 0$, and or $a_2 - a_1 \neq 0$. This is true
333   because by using the residual u_1 on the left hand side of Eq. [5c] instead of y, the parameter b_1
334   is "pulled" (i.e. should be zero in the regression) from this equation during the regression. All
335   these t tests are consistent with the estimates made of the parameters in Eq. [3d] to be discussed
336   further below.

337   As shown in the second and third columns of Table II the R^2 value is quite high at just
338   over 64%. Consequently, the chi square variable (TR^2), that test the null hypothesis of no
339   change in creep regime, is statistically significant even at the 1% significance level, meaning
340   that the null hypothesis of just one creep mechanism can be rejected. Thus, there are at least
341   two different creep mechanisms generating the minimum creep rates shown in this 1Cr - 1Mo
342   - 0.25V data set.

343   To test for the presence of a third creep mechanism, it is necessary to next construct the
344   residuals u_2 in Eq. [3d]. The last two columns of Table I shows the estimates made for the
345   parameters in Eqs. [3b,3d]. These estimates imply that the restricted residuals u_2 are given by

346        $u_2 = y - (24.4028 - 4.3613x_1 - 317.5693x_2 - 10.3971w - 1.5702wx_1 + 82.0410wx_2)$ [6b]

347   with w given by

348        $$w = \frac{1}{1 + \exp[-17.7071(x_1 - 0.4656)]}$$ [6d]

349   The last two columns of Table II shows the results obtained when u_2 is regressed on $\{1,$
350    $x_1, x_2, x^2{}_1, x^3{}_1, x^4{}_1, x_1x_2, x^2{}_1x_2, x^3{}_1x_2\}$ for the second step of the three step test procedure. It
351   reveals that none of the parameter in Eq. [5c] are statistically different from zero (even at the
352   10% significance level). It is not surprising therefore that the R^2 value is very low at just over
353   1% so that the chi square variable (TR^2), that test the null hypothesis of one change in creep
354   regime, is statistically insignificant (even at the 10% significance level). Thus the null

hypothesis of just one creep regime change cannot be comprehensively rejected. Thus, there are exactly two different creep mechanisms generating the minimum creep rates recorded within this 1Cr - 1Mo - 0.25V data set.

As briefly mentioned above, the last two columns of Table II shows the results obtained when the modified Wilshire model applied to the 1Cr - 1Mo - 0.25V data shown in Fig. 1a with two competing creep mechanisms. These estimates are slightly at odds with those originally stated by Wilshire and Scharning and as summarised in Fig. 1a. The last two columns of Table I reveals that the break appears to occur at a normalised stress of 0.47. Whilst this is slightly higher than the value provided by Wilshire and Scharning (0.4), the main differences between their results and those shown in this paper stem from the value for $\beta_1 = 17.7$ shown in Table I. This relatively low value gives rise to the sigmoidal curve shown in Fig.2. As can be seen from this figure, a transition from a low to a high stress regime occurs not instantaneously at a normalised stress of 0.47, but very gradually over a wider normalised stress range. At a normalised stress of 0.47, w in Eq. [3b] equals 0.5 implying that deformation is equally governed by two competing creep mechanisms. However, once the normalised stress falls to 0.3, deformation is predominantly determined by one of these mechanisms ($w = 0.05$ implies 95% determined) and once the normalised stress reaches about 0.6, deformation is predominantly determined by the other mechanism ($w = 0.95$ implies 95% determined). For this modified model to be equivalent to Wilshire's original specification, β_1 would need to be quite large (over 500) so that then the sigmoidal function in Fig.2 would become very step - essentially giving a very sharp and rapid transition between these two regimes.

The values for d_1 and d_2 shown in the last two columns of Table I help interpret what these competing creep mechanisms might be. At normalised stress below 0.3, w is less than 0.05 in value implying that the values for a_1, b_1 and d_1 in Eq. [3a] are predominant in describing the minimum creep rate. The value for d_1 in particular implies an activation energy of approximately 320kJmol^{-1}. At normalised stress above 0.6, w is more than 0.95 in value implying that the values for a_2, b_2 and d_2 in Eq. [3a] are predominant in describing the minimum creep rate. The value for d_2 in particular implies an activation energy of approximately 230kJmol^{-1}. Furthermore, these activation energies are statistically significantly different from each other at the 1% significance level (as shown by the student t values in the d_2-d_1 row and third column of Table I). This is consistent with the results shown in the first half of Table II which showed the parameter in front of x_1x_2 to be statistically significant - when using u_1 are the regressor variable.

This result is very different from the original Wilshire and Scharning paper where the activation was quoted to be 300kJmol^{-1} at all levels of the normalised stress. This varying activation energy must also cast doubt on their explanation for the kink in the best fit line shown in Fig.1a. For creep to occur predominantly by diffusion controlled generation and movement of dislocations within the lattice structure only, (with particle coarsening within the lattice being the cause of changing k_2 and v values), no matter what the stress level is, the activation energy should also be unchanging with respect to stress. Neither can the changing values for k_2 and v be attributable to a change from creep occurring from the generation of new dislocations within the lattice structure itself to creep occurring from the movement of

397 dislocations pre-existing in the grain boundary zones only. Because then the activation energy
398 would be lower at low normalised stress. This is not in agreement with the estimates made from
399 the data where the opposite appears to be true - the sigmoidal curve shown in Fig.3a shows the
400 activation energy increasing with decreasing normalised stresses. However, the activation
401 energies shown in Fig. 3a are consistent with the traditional view that Nabarro –Herring
402 diffusional creep becomes more dominant at lower stresses. This is further supported by the
403 fact that in the NIMS data set the lower stress tests are at the highest temperatures. If this is so,
404 then $320kJmol^{-1}$ would be that activation energy for self-diffusion. The only way to explain the
405 lower activation energy that is estimated for the high stress regime (which in the NIMS data
406 set also corresponds to low temperatures), is to suggest that under this condition the dominant
407 creep mechanism is preferential diffusion along dislocations (without dislocation movement)
408 or coble creep, i.e. stress directed vacancy flow along grain boundaries .

409   There is also a statistically significant difference between b_1 and b_2 and between a_1 and
410 a_2 as revealed by the student t values in Table I (in the a_2-a_1 and b_2-b_1 rows). Thus the gradual
411 switch in the deformation mechanism with stress is also associated with changing values for
412 both k_2 and v. In Figs. 3a,b the values for Q^*_c, k_2 and v are multiplied by the changing value
413 for w shown in Fig.2 to give an impression of how these parameters change with the normalised
414 stress. As can be seen, the main changes in the values for these parameters takes place over the
415 normalised stress range of 0.3 to 0.6. It is over this stress range then that the deformation
416 mechanism driving creep switches. These changes drive the shape of the solid curve in Fig. 3a.
417 Along the stretch a – b we have the familiar negative relationship between $\ln(-\ln(\sigma/\sigma_T s)$ and
418 $\ln[\dot{\varepsilon}_m . \exp\{Q^*_c/RT\}]$. Then Q^*_c starts to change rapidly and this leads to the stretch of the curve
419 between b and c. Finally, over the normalised stress range 0.1 - 0.3, the familiar negative
420 relationship between $\ln(-\ln(\sigma/\sigma_T s)$ and $\ln[\dot{\varepsilon}_m . \exp\{Q^*_c/RT\}]$ returns but now the activation
421 energy is much higher than before.

B.   2.25Cr-1Mo steel

423   In order to apply the sequential testing procedure described in section III above to the
424 2.25Cr-1Mo data shown in Fig. 1b, it is necessary to first construct the residuals u_1 in Eq. [2].
425 Columns two and three of Table III shows the estimates made for the parameters in Eq. [2].
426 The t values show that parameters b and d are statistically significant at the 1% significance
427 level with the value for d implying an activation energy of nearly $200kJmol^{-1}$. These estimates
428 imply that the residuals u_1 are given by

429      $u_1 = y - (7.4906 - 6.1446x_1 - 190.2616x_2)$ [7a]

430   Columns 2 and 3 of Table IV show the results obtained when u_1 is then regressed on
431 $\{1, x_1, x_2, x^2_1, x^3_1, x^4_1, x_1x_2, x^2_1x_2, x^3_1x_2\}$ for the second step of the three step test procedure. It
432 reveals that at the 5% significance level, the only parameter to be statistically insignificant is
433 that in front of x^4_1 in Eq. [5c]. Eq. [5c] also suggests that this result can only be so if there is a
434 statistically insignificant change in the value for v in Eq. [2] (as then b_2 - b_1 = 0). Eq. [5c] also
435 suggests that the statistical significance of all the other parameters shown in these two columns
436 can only be so if there is a statistically significant change in both d_1 and a_1. Then a_2 - $a_1 \neq 0$

437 (leading to the parameter in front of x_1, x^2_1 and x^3_1 in the first half of Table IV being significantly
438 different from zero), and $d_2 - d_1 \neq 0$ (leading to the parameter in front of $x_1 x_2$ in the first half of
439 Table IV being significantly different from zero). All these t tests are consistent with the
440 estimates made of the parameters in Eq. [3d] to be discussed further below.

441 As shown in columns two and three of Table IV, the R^2 value is quite high at just over
442 91%, so that the chi square variable (TR^2), that test the null hypothesis of no change in creep
443 regime, is statistically significant even at the 1% significance level. This in turn means that the
444 null hypothesis of just one creep mechanism is rejected by the data. Thus, there are at least two
445 different creep mechanisms generating the minimum creep rates recorded in this 2.25Cr-1Mo
446 data set.

447 To test for the presence of a third creep mechanism, it is necessary to next construct the
448 residuals u_2 in Eq. [3d]. The middle section of Table III shows the estimates made for the
449 parameters in Eq. [3d]. These estimates imply that the residuals u_2 are given by

450 $$u_2 = y - (6.5490 - 4.8317x_1 - 198.9690x_2 + 29.4426w + 0.0727wx_1 - 165.6330wx_2) \qquad [7b]$$

451 with w given by

452 $$w = \frac{1}{1 + \exp[-38.6887(x_1 - 0.2638)]} \qquad [7c]$$

453 The last two columns of Table IV show the results obtained when u_2 is regressed on $\{1,$
454 $x_1, x_2, x^2_1, x^3_1, x^4_1, x_1x_2, x^2_1x_2, x^3_1x_2\}$ for the second step of the three step test procedure. It
455 reveals, first of all, that the parameter in front of x^4_1 is statistically different from zero at the
456 5% significance level. Eq. [5c] also suggests that this can only be so if there is a statistically
457 significant change in the slope of the best fit line in Fig. 1b (as then $b_2 - b_1 \neq 0$). The statistical
458 significance of the parameter in front of x^2_1 at the 5% significance level may also indicate that
459 the intercept of the best fit line in Fig. 1b changes (as then $a_2 - a_1 \neq 0$). The last two columns
460 Table IV also reveals the parameter in front of $x^2_1x_2$ is statistically different from zero at the
461 10% significance level. Eq. [5c] also suggests that this can only be so if there is a statistically
462 significant change in the activation energy (as then $d_2 - d_1 \neq 0$). These t statistics are therefore
463 suggestive that for this material at least three creep mechanisms are at work. This is further
464 confirmed by the R^2 value, which is quite high at just over 34% so that the chi square variable
465 (TR^2), that test the null hypothesis of just two creep regimes, is statistically significant at the
466 10% significance level. This in turn means that the null hypothesis of just two creep mechanism
467 is rejected by the data. Thus, there are at least three different creep mechanisms generating the
468 minimum creep rates recorded in this 2.25Cr - 1Mo steel data set.

469 Although the results of testing the null hypothesis of exactly three creep regimes using
470 this LM test are not shown here, the test leads to the acceptance of this null hypothesis - even
471 at the 10% significance level. Thus for this material there appears to be three distinctly different
472 creep regimes or mechanisms and the parameter estimates of Eq. [4b,c] shown in the last two
473 columns of Table III throw some light on the nature of these regimes. These estimates are
474 slightly at odds with those originally stated by Wilshire and Whittaker - which are shown in

475 Fig. 1b. The last two columns of Table III reveals that the two break points appear to occur at
476 normalised stresses of 0.26 and 0.42. Whilst these are slightly different to the values provided
477 by Wilshire and Whittaker (around 0.1 and 0.5 respectively), the main difference stems from
478 the values for $\beta_1 = 50.5$ and $\beta_3 = 18.1$ shown towards the bottom of Table III. These values
479 give rise to the sigmoidal and bell shaped curves shown in Fig.4.

480   As can be seen from this figure, a transition from a low to a medium stress regime and
481 then from a medium to a high stress regime occurs, but not instantaneously, at normalised
482 stresses of 0.26 and 0,42 respectively. Below a normalised stress of 0.3, about 90% of the
483 deformation is governed by the first creep mechanism (summarised by the value for w_1). The
484 remaining deformation is governed by the other two mechanisms. Then at a normalised stress
485 of around 0.30 the second mechanism dominates with about 80% of the deformation being
486 controlled by this mechanism (as shown by the value for w_2). Beyond a normalised stress of
487 0.42, the third mechanism starts to dominate with around 90% of the deformation being
488 governed by this last mechanism at normalised stresses of 0.55 and above (as reflected in the
489 value for w_3). For this modified model to be equivalent to Wilshire and Whittaker's original
490 specification, β_1 and β_3 would need to be quite large (over 500) so that then the sigmoidal
491 functions in Fig.4 would become very step, and the bell shaped function very compressed,-
492 essentially giving a very sharp and rapid transition between the regimes.

493   The values for d_1, d_2 and d_3 in the last two columns of Table III help interpret what
494 these competing creep regimes or mechanisms might be. At a normalised stress around 0.30,
495 w_2 is about 0.8 in value implying that the values for a_2, b_2 and d_2 in Eq. [4b] are predominant
496 in describing deformation and the minimum creep rate. The value for d_2 then implies an
497 activation energy of approximately 240kJmol^{-1} which is consistent with the estimates made by
498 Wilshire and Whittaker for this middle stress regime (see Fig. 1b where the activation energy
499 is given by the authors at 230kJmol^{-1}). At normalised stresses less than 0.2, w_1 is 0.8 or more
500 in value implying that the values for a_1, b_1 and d_1 in Eq. [4b] are predominant in describing
501 deformation and the minimum creep rate. The value for d_1 shown in the last two columns of
502 Table III then implies an activation energy of approximately 200kJmol^{-1}, but because the t
503 statistic on d_1-d_2 is insignificant (implying d_1-d_2 is insignificantly different from zero), the
504 conclusion must be that the activation energy in this low stress regime is not different to that
505 in the medium stress regime. This is very different to the conclusion given by Wilshire and
506 Whittaker who maintain that the activation energy is much higher in this low stress regime (but
507 they provide no statistical proof for this hypothesis). At normalised stresses above 0.55, w_3 is
508 0.8 or more in value implying that the values for a_3, b_3 and d_3 in Eq. [4b] are predominant in
509 describing deformation and the minimum creep rate. The value for d_3 shown in Table III then
510 implies an activation energy of approximately 400kJmol^{-1}, and because the t statistic on d_3-d_2
511 is statistically significant, the conclusion must be that the activation energy in this high stress
512 regime is different to that in both the medium and low stress regimes. This activation energy is
513 much higher than that quoted by Wilshire and Whittaker who maintain that the activation
514 energy is around 280kJmol^{-1} in this high stress regime (see Fig. 1b).

515   According to Wilshire and Whittaker [5], when $\sigma > \sigma_Y$, creep is controlled by the
516 generation and movement of dislocations within the grains. This would require a high

activation energy, which is consistent with the result described above where an activation energy is estimated at around 400kJmol^{-1}. In contrast, when $\sigma < \sigma_Y$, Wilshire and Whittaker suggest that dislocations are not generated within the grains. Instead, creep occurs within the grain boundary zones, i.e. by grain boundary sliding and or diffusion along existing dislocations and grain boundaries. This requires a lower activation energy, which is consistent with the result described above where an activation energy of around 230kJmol^{-1} is estimated for medium stresses. Wilshire and Whittaker then suggest another change in creep and creep rupture behaviour occurs when σ approximately equals $0.2\sigma_{TS}$. With this material, they suggest the original ferrite/bainite microstructure degrades to ferrite and molybdenum carbide particles in long term tests at the highest creep temperatures, with very coarse carbide particles forming along the grain boundaries (which takes place in long-term tests at the highest creep temperatures). This then enables deformation to once again be determined by processes within the lattice structure, where the activation energy is greatest. Whilst the results in this paper suggest that a mechanism change does indeed occur in the transition from medium to very low stresses, there is no significant increase in the activation energy. Contrary to the Wilshire explanation, this result suggests that creep is not predominantly determined by processes occurring within the lattice structure material - because the activation energy is highest within the bulk. It would seem instead that sliding and or diffusion along existing dislocations and grain boundaries still predominates at these very low stresses. But that the coarsening of the carbide particles reduces creep strength further given the different stress relation shown in the low stress regime compared to the medium stress regime, i.e. allows creep rates to be much higher than would be predicted using relations that apply in the medium stress regime.

There are also statistically significant differences between b_1, b_2 and b_3 and between a_1, a_2 and a_3 as revealed by the student t values in Table III (in the a_1-a_2, a_3-a_2 and the b_1-b_2, b_3-b_2 rows). Thus the gradual switch in deformation mechanisms with stress is also associated with changing values for both k_2 and v. In Figs. 5a,b the values for Q^*_c, k_2 and v are multiplied by the changing value for w_i shown in Fig. 4 to give an impression of how these parameters change with the normalised stress. As can be seen, the main changes in the values for these parameters takes place over the normalised stress range of 0.2 to 0.5. k_2 appears to continually increase with the normalised stress, whilst v is similar in value at the highest and lowest stresses with a temporary increase over the intermediate normalised stress ranges. The values for v at the end points (i.e. at points a and d in Fig. 5a) are very similar to the estimates made by Wilshire and Whittaker in their original study – as can be seen by a comparison of Fig.1a with Fig.5a. However, the values for k_2 in this study appear a little larger in comparison.

Finally, the solid curves in Fig.6 shows what the predictions given in Fig.5 look like in stress - minimum creep rate space. It can be seen that the predictions trace out well defined smooth curves as the stress level varies. In contrast to this, the dotted "curves" show the predictions obtained when the weighting functions w_1 to w_3 are step like in nature which then closely corresponds to the original Wilshire – Whittaker specification for this material. The predictions at some of the temperatures are very discontinuous due to abrupt changes in the activation energy and the functional relationship of the minimum creep rate with stress. These discontinuities do not make physical sense and lead to rather bizarre behaviour. For example,

559   at 873K (600°C) and between 53 MPa and 41 MPa, the minimum creep rate slows down in a
560   uniform fashion, but then just before a stress of 41 MPa is reached the model predicts the creep
561   rate will suddenly increase even though there has been little change in the stress level. From a
562   creep perspective this makes little sense and reflects the incorrect specification of the way the
563   activation energy changes with stress (in reality it is gradual rather than abrupt).

V.   CONCLUSIONS

565   This paper has put forward a statistical test for determining the correct number of
566   discontinuities to use within the Wilshire equations and also a method for allowing these
567   discontinuities to change more gradually with the normalised stress level - so that the
568   methodology is more in line with the accepted view as to how creep mechanism evolve with
569   changing test conditions. The new findings obtained using this modified methodology include:

570   i.   In their study of 1Cr - 1Mo - 0.25V steel, Wilshire and Scharning worked with a constant
571   activation energy of 300kJmol^{-1} and a change in the relationship between the minimum
572   creep rate and the normalised stress that occurred abruptly at a normalised stress of 0.4.
573   In contrast, this paper found that the activation energy also changed with the normalised
574   stress. Further, these changes occurred gradually over a normalised stress range of around
575   0.3 to 0.6. This changing activation energy in turn casts doubt on the authors view that
576   the changing values for k_2 and v were the result of particle coarsening associated with
577   long test durations at lower stresses.
578   ii.   In their study of 2.25Cr-1Mo Wilshire and Whittaker worked with an activation energy
579   that was lower for mid-range normalised stresses (230kJmol^{-1}) than it was for any other
580   value of the normalised stress (where they took the activation energy to be 280kJmol^{-1}).
581   In contrast, this paper found the activation energy to be around 400kJmol^{-1} at the highest
582   values for the normalised stress but around 240kJmol^{-1} for all other values of the
583   normalised stress. These difference suggest that creep is not predominantly determined
584   by processes occurring within the lattice structure at these lowest stress values as
585   originally suggested by these authors. Over the normalised stress range 0.2 to 0.5, creep
586   is predominantly determined by a single process with an activation energy of 240kJmol^{-1}
587   . Below a normalised stress of 0.25, there is quite an abrupt change in the values for k_2
588   and v, whilst in contrast, the changes in k_2 and v are more gradual for increases in the
589   normalised stress above a value of 0.45.
590   iii.   When the new procedures outlined in this paper were applied to 2.25Cr-1Mo steel, they
591   produce more accurate and realistic looking long term predictions of the minimum creep
592   rate.

593   An important area for future work includes applying the methodology outlined in this
594   paper to other steel alloys to confirm whether this approach also produced better long term
595   predictions for these materials, and better understanding of the changing deformation
596   mechanisms.

597

598

599

600

601

REFERENCES

1. ASME Boiler & Pressure Vessel Code, Sec. II, Part D, Appendix I, ASME, 2004.

2. D. Allen and S. Garwood: *Materials Energy Review*, IoMMH, London, 2007.

3. B. Wilshire and A.J. Battenbough: *Materials Science and Engineering A,* 2007, 443, pp. 156-166.

4. B. Wilshire and P.J. Scharning: *Materials Science and Technology*, 2008, 24(1), pp. 1-9.

5. B. Wilshire, and M. Whittaker: *Materials Science and Technology*, 2011, 27(3), pp. 642-647.

6. B. Wilshire and P.J. Scharning: *International Materials Reviews*, 2008, 53(2), pp. 91-104.

7. A. Abdallah, K. Perkins and S. Williams: *Materials Science and Engineering A*, 2012, 550, pp. 176-182.

8. M.T. Whittaker, M. Evans and B. Wilshire: *Materials Science and Engineering A*, 2012, 552, pp. 145-150.

9. National Institute for Materials Science, Creep Data Sheet No. 9b: Data sheets on the elevated-temperature properties of $1Cr - 1Mo - 0.25$ steel forgings for rotors and shafts, 1990.

10. National Institute for Materials Science, Creep Data Sheet No. M-6: Metallographic atlas of long term crept materials, 2007.

11. National Institute for Materials Science, Creep Data Sheet No. 3b: Data sheets on the elevated-temperature properties of $2.25Cr - 1Mo$ steel, 1986.

12. H. Tong: Threshold models in non-linear time series analysis. *Lecture Notes in Statistics 21*. Springer-Verlag, 1983.

13. V. Martin, S. Hurn and D. Harris. *Econometric Modelling with Time Series: Specification, estimation and testing,* Cambridge University Press, Cambridge, 2013, *Chapter 19*.

14. M. Evans: *Metallurgical and Materials Transactions A*, 2015, Volume 46, Issue 2, pp. 937-947.

15. G. Vinning and S.M. Kowalski: *Statistical Methods for Engineers,* 3rd Ed., Brooks/Cole, Boston, 2011, Chapter 6.

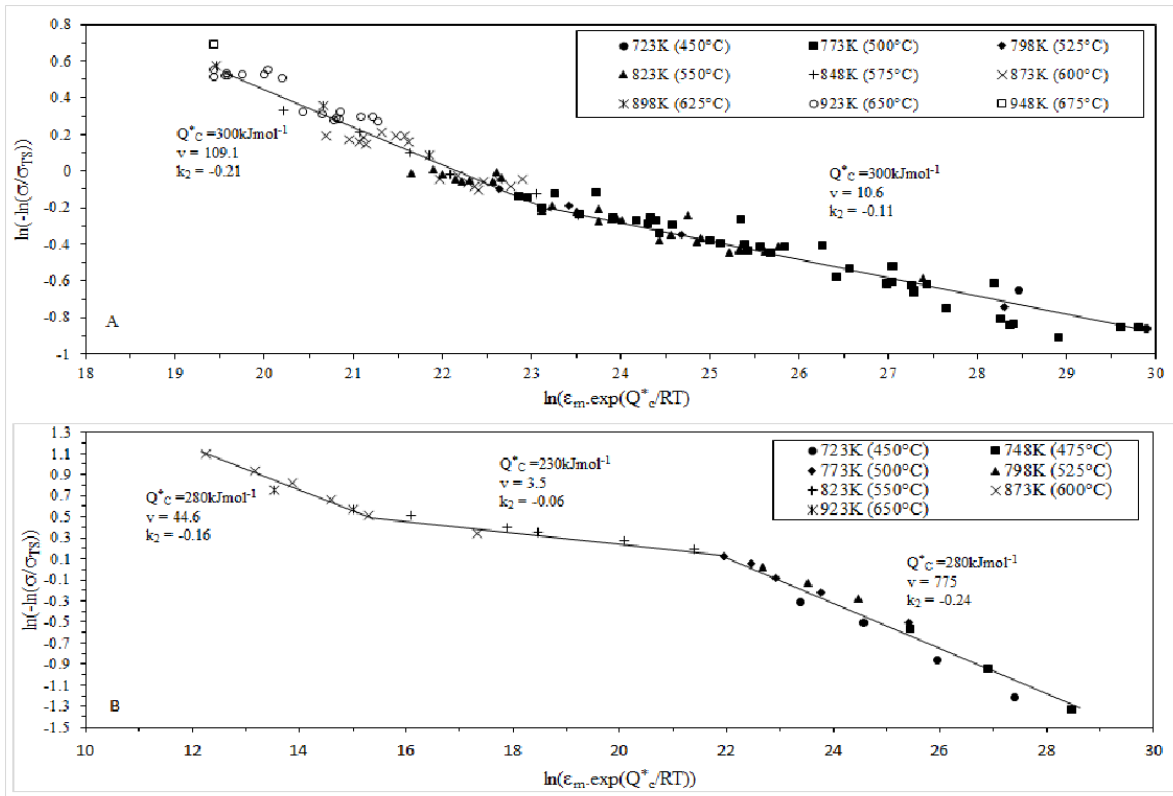16. R. Luukkonen, P. Saikkonen and T. Terasvirta: *Biometrica,* 1988, 75, pp. 491-499.

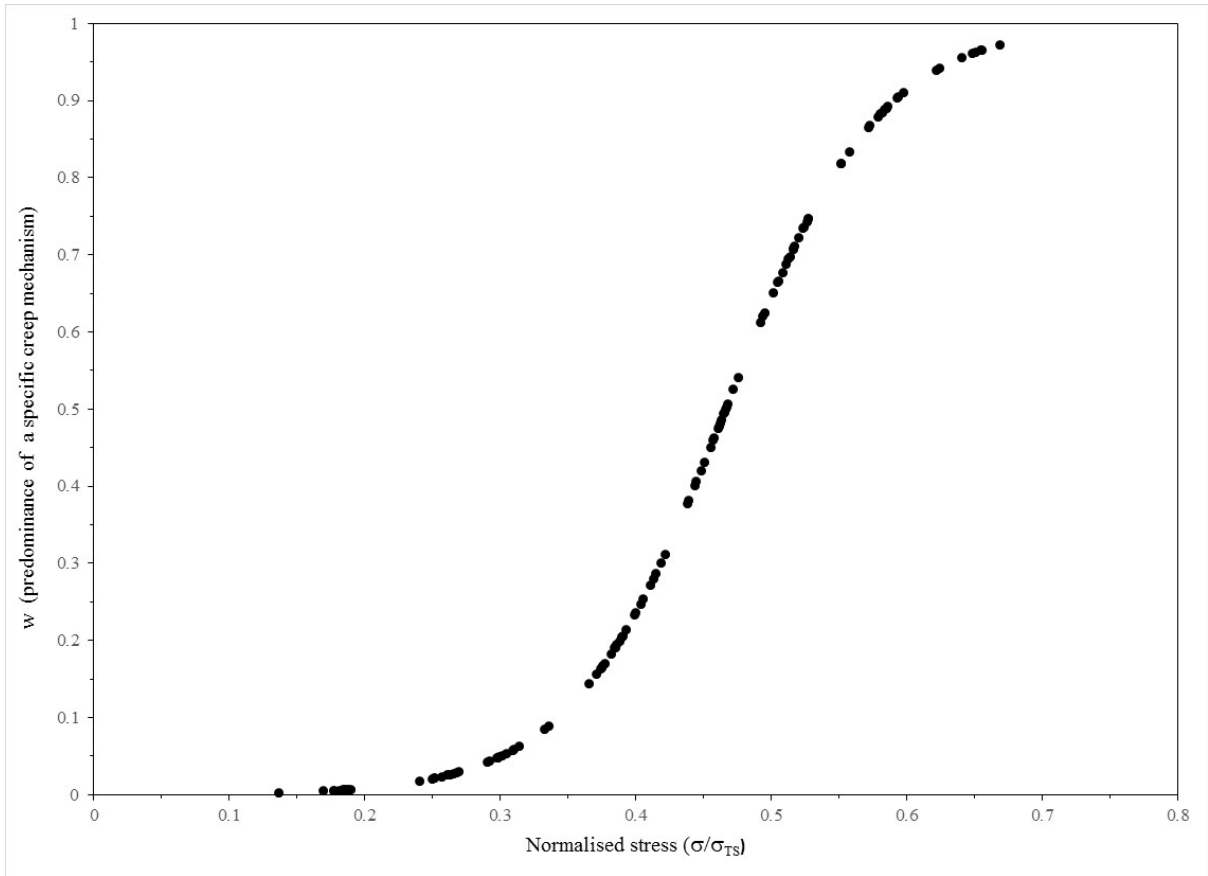17. B.E. Hansen: *Econometrica,* 1996, 50, pp. 1269-1286.

18. T.H. Lee, H. White and C.W.J. Granger: *Journal of Econometrics*, 1993,5 6, pp. 269-290.

Fig.1 – The best values for k_2, v and Q^*_c determined by Wilshire and Scharning[4] and Wilshire and Whittaker[5] were found by plotting $\ln[\varepsilon_m.\exp(Q^*_c/RT)]$ against $\ln(-\ln(\sigma/\sigma_{TS}))$ for a. 1Cr - 1Mo – 0.25 steel forgings for rotors and shafts and b. for 2.25Cr-1Mo steel tubes.

645

646 Fig. 2 - The dominance of two different deformation mechanisms at different stresses for 1Cr-
647 1Mo-0.25V steel.
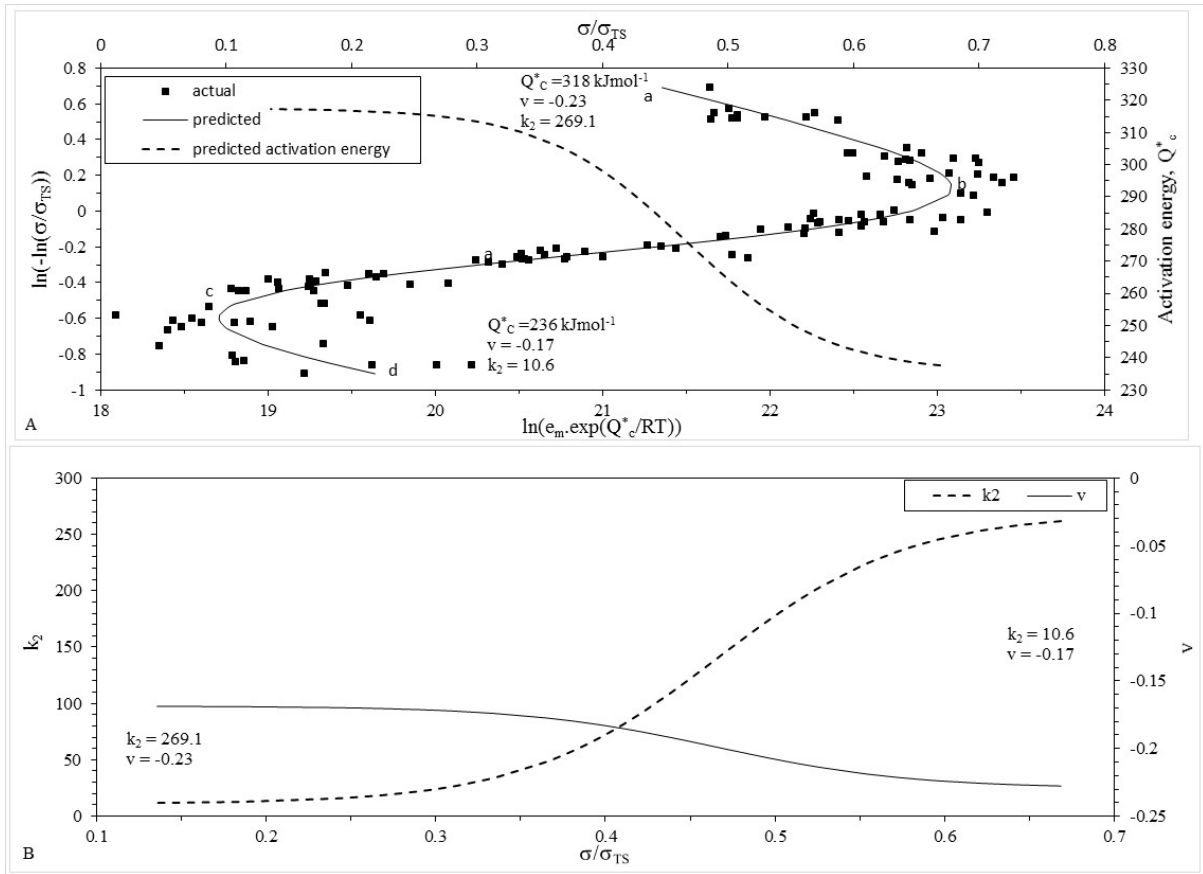
Fig.3 – Dependence of a. $\ln[\varepsilon_m.\exp(Q^*_c/RT)]$ on $\ln(-\ln(\sigma/\sigma_{TS}))$ and the activation energy on the normalised stress and b. dependence of k_2 and v on the normalised stress for 1Cr-1-Mo-0.25V steel at various temperatures.
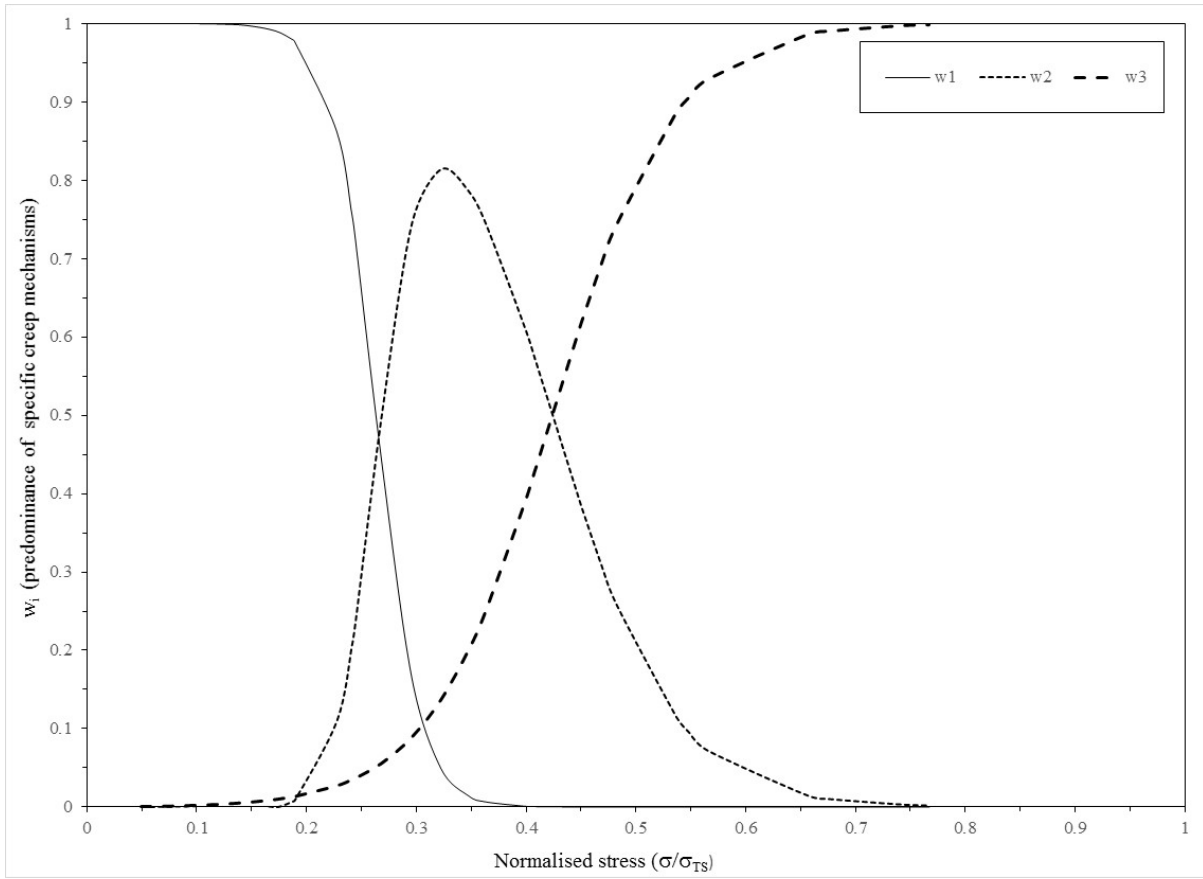
652

653 Fig. 4 - The dominance of three different deformation mechanisms at different stresses for
654 2.25Cr-1Mo steel.
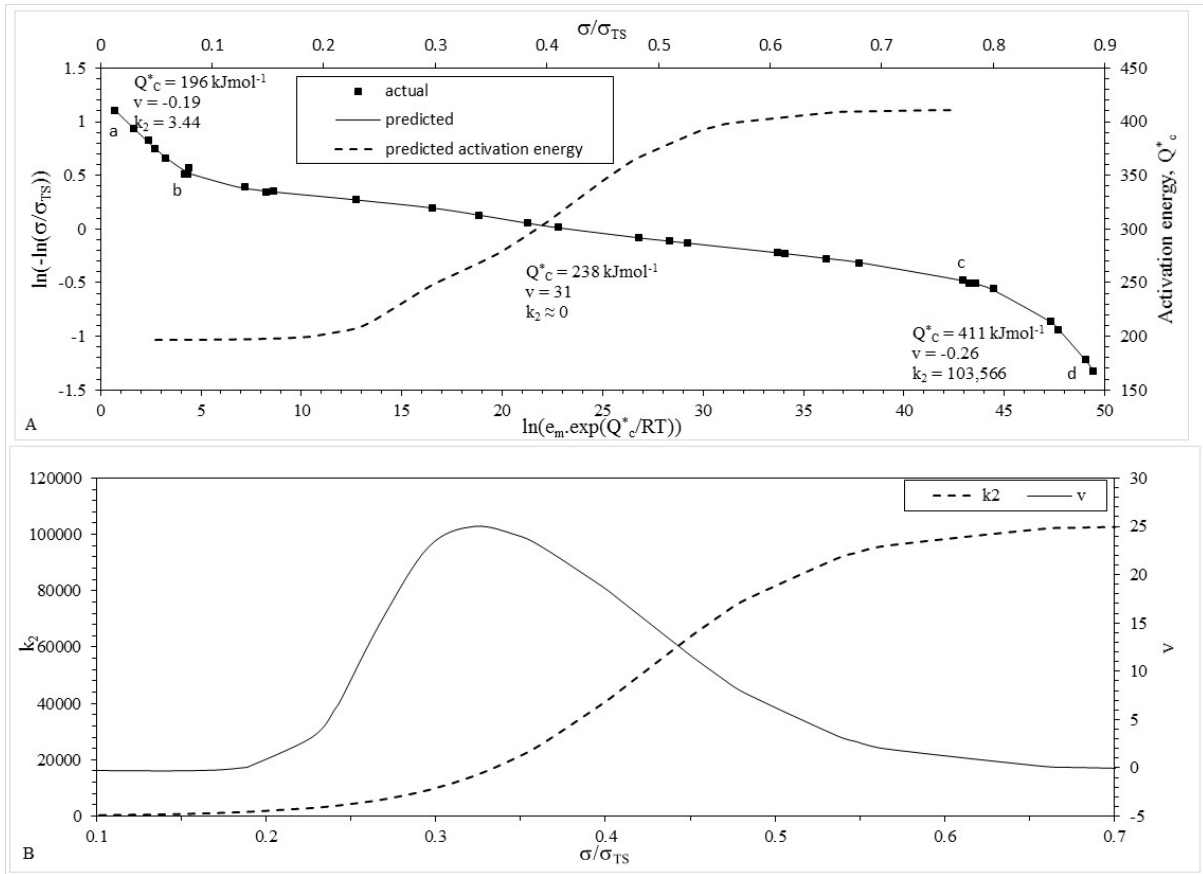
Fig.5 – Dependence of a. $\ln[\varepsilon_m.\exp(Q^*_c/RT)]$ on $\ln(-\ln(\sigma/\sigma_{TS}))$ and the activation energy on the normalised stress and b. dependence of k_2 and v on the normalised stress for 2.25Cr-1Mo steel at various temperatures.
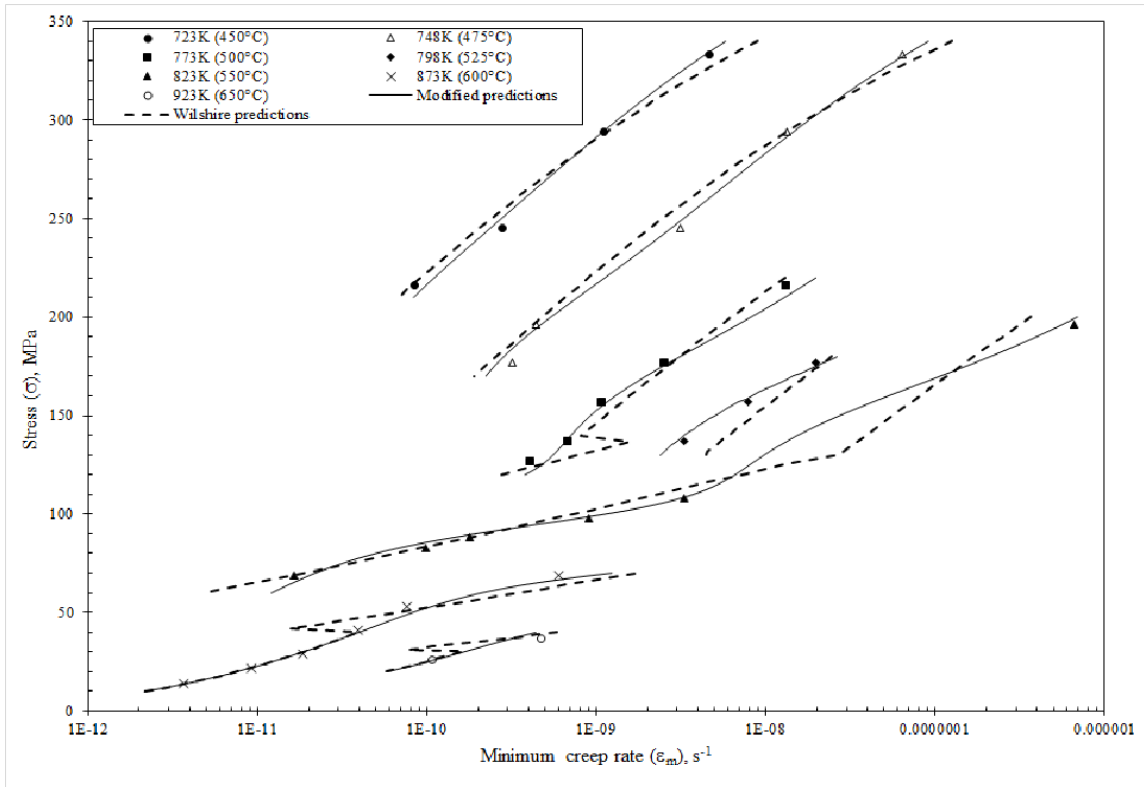
659

660 Fig.6 – Minimum creep rates in 2.25Cr-1Mo steel tubes predicted by the modified and original
661 specifications of the Wilshire equation.

662

663

664

665

666

667

668

669

670

671

672

673

674

Table I. Least Squares Estimates for the Parameters in Eq. [2] and Eqs. [3b,3d] when using
1Cr-1Mo-0.25V Steel Forging Data

Parameters	Eq. [2]		Eqs. [3b,3d]	
	Least squares estimates	t value	Least squares estimates	t value
a	23.2390	14.43***	-	-
b	-6.9101	-24.24***	-	-
d	-304.4505	-26.89***	-	-
a_1	-	-	24.4028	13.22***
b_1	-	-	-4.3613	-10.09***
d_1	-	-	-317.5693	-24.44***
a_2-a_1	-	-	-10.3971	-2.91***
b_2-b_1	-	-	-1.5702	-2.67***
d_2-d_1	-	-	82.0411	3.34***
a_2	-	-	14.0057	6.06***
b_2	-	-	-5.9316	-11.35***
d_2	-	-	-235.5282	-8.47***
x^*_1	-	-	0.4656	-
β_1	-	-	17.7071	-

- Parameters are not part of the model.
***Parameters are statistically different from zero at the $\alpha = 1\%$ and above significance level.
**Parameters are statistically different from zero at the $\alpha = 5\%$ and above significance level.
*Parameters are statistically different from zero at the $\alpha = 10\%$ and above significance level.
T is the sample size (T=121).
t has a student t distribution with T - 3 degrees of freedom for Eq. [2] and T - 6 degrees of freedom for Eq. [3d].

681 **Table II.** Results from Regressing u_1 and u_2 on $\{1, x_1, x_2, x^2{}_1, x^3{}_1, x^4{}_1, x_1x_2, x^2{}_1x_2, x^3{}_1x_2\}$
682 when using 1Cr-1Mo-0.25V Steel Forging Data

Variable	u_1 Least squares estimates	u_1 t & Chi square values	u_2 Least squares estimates	u_2 t & Chi square values
Constant	-0.9344	-0.54	-0.7656	-0.45
x_1	14.8038	2.51**	0.8635	0.15
x_2	2.9373	0.24	5.3381	0.44
$x^2{}_1$	6.3926	0.38	17.1725	1.01
$x^3{}_1$	-0.3812	-0.02	17.3221	0.82
$x^4{}_1$	-4.1614	-1.17	-2.7544	-0.78
x_1x_2	-98.4011	2.31**	-5.6813	-0.13
$x^2{}_1x_2$	-25.0805	-0.21	-122.0521	-1.03
$x^3{}_1x_2$	-7.2728	-0.04	-139.0271	-0.85
R^2 (%)	64.17	-	1.03	-
LM = TR^2	-	77.68***	-	1.25

***Parameters are statistically different from zero at the $\alpha = 1\%$ and above significance level. **Parameters are statistically different from zero at the $\alpha = 5\%$ and above significance level. *Parameters are statistically different from zero at the $\alpha = 10\%$ and above significance level.

R^2 is the coefficient of determination or the percentage variation in u explained by all the variables shown in the first column of the table.

TR^2 has a chi square distribution with 6 degrees of freedom. T is the sample size (T = 121). t has a student t distribution with T - 9 degrees of freedom.

683

684

685

686

687

688

689

Table III. Least Squares Estimates for the Parameters in Eq. [2] and Eqs. [3b,3d] when using 2.25Cr - 1Mo Steel Tube Data

Parameters	Eq. [2] Estimate	Eq. [2] t value	Eq. [3d] Estimate	Eq. [3d] t value	Eq. [4b,c] Estimate	Eq. [4b,c] t value
a	7.4906	1.15	-	-	-	-
b	-6.1446	-7.99***	-	-	-	-
d	-190.2616	-4.38***	-	-	-	-
a_2	-	-	-	-	15.6319	3.16***
b_2	-	-	-	-	0.0325	0.02
d_2	-	-	-	-	-238.3443	-7.45***
a_1-a_2	-	-	-29.4426	-7.58***	-8.9704	-1.65*
a_3-a_2	-	-	-	-	28.8024	4.43***
b_1-b_2	-	-	-0.0727	0.14	-5.422	-3.81***
b_3-b_2	-	-	-	-	-3.8803	-2.98***
d_1-d_2	-	-	165.6330	6.33***	42.1756	1.18
d_3-d_2	-	-	-	-	-172.4897	-4.18***
a_1	-	-	6.5419	2.06**	6.6615	19.24***
a_3	-	-	-	-	44.3426	3.18***
b_1	-	-	-4.8317	-9.59***	-5.3897	-12.28***
b_3	-	-	-	-	-3.8478	-15.54***
d_1	-	-	-198.9690	-9.05***	-196.1688	-6.58***
d_3	-	-	-	-	-410.8314	-28.42***
x^*_1	-	-	0.2638	-	0.2638	-
β_1	-	-	38.6887	-	50.5172	-
x^{**}_1	-	-	-	-	0.4239	-
β_3	-	-	-	-	18.1292	-

- Parameters are not part of the model.
***Parameters are statistically different from zero at the $\alpha = 1\%$ and above significance level.
**Parameters are statistically different from zero at the $\alpha = 5\%$ and above significance level.
*Parameters are statistically different from zero at the $\alpha = 10\%$ and above significance level.
T is the sample size (T = 31).
t has a student t distribution with T-3 degrees of freedom for Eq. [2] and T - 6 degrees of freedom for Eq. [3d].

692

693

694

695

696

698 **Table IV.** Results from Regressing u_1 and u_2 on $\{1, x_1, x_2, x^2_1, x^3_1, x^4_1, x_1x_2, x^2_1x_2, x^3_1x_2\}$
699 when using 2.25Cr - 1Mo Steel Tube Data

Variable	u_1		u_2	
	Least squares estimates	t & Chi square values	Least squares estimates	t& Chi square values
Constant	10.8126	2.80**	3.1162	-1.35
x_1	-50.3627	-6.05***	-7.7382	-1.55
x_2	-62.4319	-2.47**	20.0285	1.32
x^2_1	22.5831	12.09***	14.9435	2.07**
x^3_1	47.5139	3.63***	5.7176	0.72
x^4_1	-0.9135	-0.84	-1.3998	-2.13**
x_1x_2	315.8915	5.60***	51.5805	1.53
$x^2_1x_2$	-162.0437	-2.09**	-88.0569	-1.90*
$x^3_1x_2$	-314.1496	-3.45***	-44.4357	-0.83
R^2 (%)	91.03	-	34.25	-
TR^2	-	28.22***	-	10.72*

***Parameters are statistically different from zero at the α = 1% and above significance level. **Parameters are statistically different from zero at the α = 5% and above significance level. *Parameters are statistically different from zero at the α = 10% and above significance level.
R^2 is the coefficient of determination or the percentage variation in u explained by all the variables shown in the first column of the table.
TR^2 has a chi square distribution with 6 degrees of freedom. T is the sample size (T = 31). t has a student t distribution with T - 9 degrees of freedom.

700